J Mater Sci (2008) 43:5705–5711
DOI 10.1007/s10853-008-2902-9

Effect of thermomechanical processing on mechanical behavior and microstructure evolution of C–Mn multiphase high strength cold rolled steel

Élida G. Neves · Ronaldo N. Barbosa · Elena V. Pereloma · Dagoberto B. Santos

Received: 27 February 2008 / Accepted: 23 July 2008 / Published online: 13 August 2008

Abstract Multiphase (MP) steels have complex microstructures containing polygonal ferrite, martensite, bainite, carbide, and small amounts of retained austenite. This mixture of phases and constituents is responsible for a good combination of strength and ductility in this class of steels. The present work shows how different annealing parameters can be used to create the suitable microstructure to improve mechanical properties of MP steels. Samples were first heated to 740, 760, or 780 °C, held for 300 s, and then quickly cooled to 600 or 500 °C. They were then soaked for another 300 s and finally accelerated cooled in the range of 10–30 °C s^{-1}. The microstructures were examined at the end of each processing route using optical, scanning, and transmission electron microscopy. Hardness values were determined for all conditions. Analysis of the available data allowed to establish the simple and yet useful quantitative relationship between the microstructural parameters, cooling rates, and hardness of the steel.

É. G. Neves · R. N. Barbosa · D. B. Santos (✉)
Department of Metallurgical and Materials Engineering, Federal University of Minas Gerais, R. Espirito Santo, 35-s206-Centro, Belo Horizonte 30160.030, MG, Brazil
e-mail: dsantos@demet.ufmg.br

É. G. Neves
e-mail: elidaneves@yahoo.com.br

R. N. Barbosa
e-mail: rbarbosa@demet.ufmg.br

E. V. Pereloma
BlueScope Steel Metallurgy Centre, Faculty of Engineering, School of Mechanical, Materials and Mechatronics Engineering, University of Wollongong, Northfields Avenue, Wollongong, NSW 2522, Australia
e-mail: elenap@uow.edu.au

Introduction

The use of traditional light weight materials, such as aluminum, magnesium, or even relatively new ones, such as advanced polymers and carbon fibers, has been considered as replacement for steel in many applications. This forced automakers to increase demands for alloys with higher strength, toughness, and deep drawing performances as compared to materials available in those days [1, 2]. However, steel continues to be an excellent candidate for automotive applications, since higher strengths combined with other desirable properties, such as extraordinary fatigue resistance or formability, are achievable. In addition, the production of steels requires, in general, relatively low energy consumption and at the end of a product life recycling costs are also low. Technology is available nowadays to produce low cost steels with high mechanical strength, better formability, high energy absorption capacity, high toughness, and enhanced corrosion resistance. This has been achieved, nonetheless, by using lean compositions similar to those found in low C steels. In this way, general production costs are not increased leading to an improvement in productivity.

The applications of high strength steels in the automotive industry are centered on dual phase (DP), transformation-induced plasticity (TRIP), and multiphase (MP) steels. The latter is the subject of this work. The microstructure of MP steels consists of bainite, martensite, a small amount of retained austenite and carbides [3–5]. Depending on the volume fractions of martensite and bainite present, different classes of strength can be obtained, although this comes with the loss in ductility. The 600 MPa tensile strength steel class, for instance, contains 80–90% of ferrite with the remainder being martensite. However, this steel can have a tensile strength ranging from 700 to

900 MPa and yet retain considerable total elongation, in the range of 15–25%, if suitable processing route is employed [2–5].

In this work, a series of thermal cycles were used to simulate continuous annealing production of complex MP steels. The purposes of the experiments were to understand the effect of processing route on, first, the microstructure formation and, second, the effects of these microstructures on hardness.

Experimental procedure

Low C high Mn steel with the following composition: 0.08C, 1.91Mn, 0.04 Si, 0.018P, 0.006S, 0.035Al, and 0.005 N, (wt.%) was used in the experiments. The as-received material was a hot-rolled coil with the microstructure predominantly containing ferrite/pearlite. The hot rolling coils were then cold rolled to a total reduction of 66% reaching 1.23 mm thickness. Ribbons of $1.23 \times 20.0 \times 45.0$ mm^3 were cut parallel to the rolling direction from the strip for simulations of continuous annealing. The microstructure of these samples consisted of work hardened ferrite and pearlite. Simulation of continuous annealing took place first by intercritical annealing of the samples followed by isothermal transformation and finally by accelerated cooling of the samples to room temperature. The temperatures chosen for intercritical annealing (T_{IA}) were 740, 760, or 800 °C. After soaking for 300 s at these temperatures, the specimens were cooled at a 5 °C s^{-1} cooling rate to intermediate temperatures of 500 or 600 °C (T_{IH}). Afterward, the specimens were cooled down to room temperature using average cooling rates, ranging from 10 to 30 °C s^{-1}. Details of the simulation process are given in Fig. 1 [6]. During the initial heating, the samples were recrystallized, as also reported elsewhere [7]. Temperatures of phase transformations on heating and cooling were estimated using well-known equations for bainite and martensite formation [3, 8]. The time spent to achieve the isothermal hold temperature of 600 or 500 °C varied from approximately 80–110 s, respectively (Fig. 1b). The rates employed during fast cooling were averaged by measuring between 2 and 10 s for the slow and intermediate cooling rate experiments and between 2 and 5 s for the cooling at approximately 30 °C s^{-1} (Fig. 1c), the last step displayed in Fig. 1a.

Optical microscopy was carried out using conventional methods. Both longitudinal and transverse cross sections were examined. LePera [7] and 2% nital etchings were used for the analysis.

Scanning electron microscopy (SEM) images were obtained using a JEOL JSM 6360LV microscope with THERMO NORAN QUEST EDS.

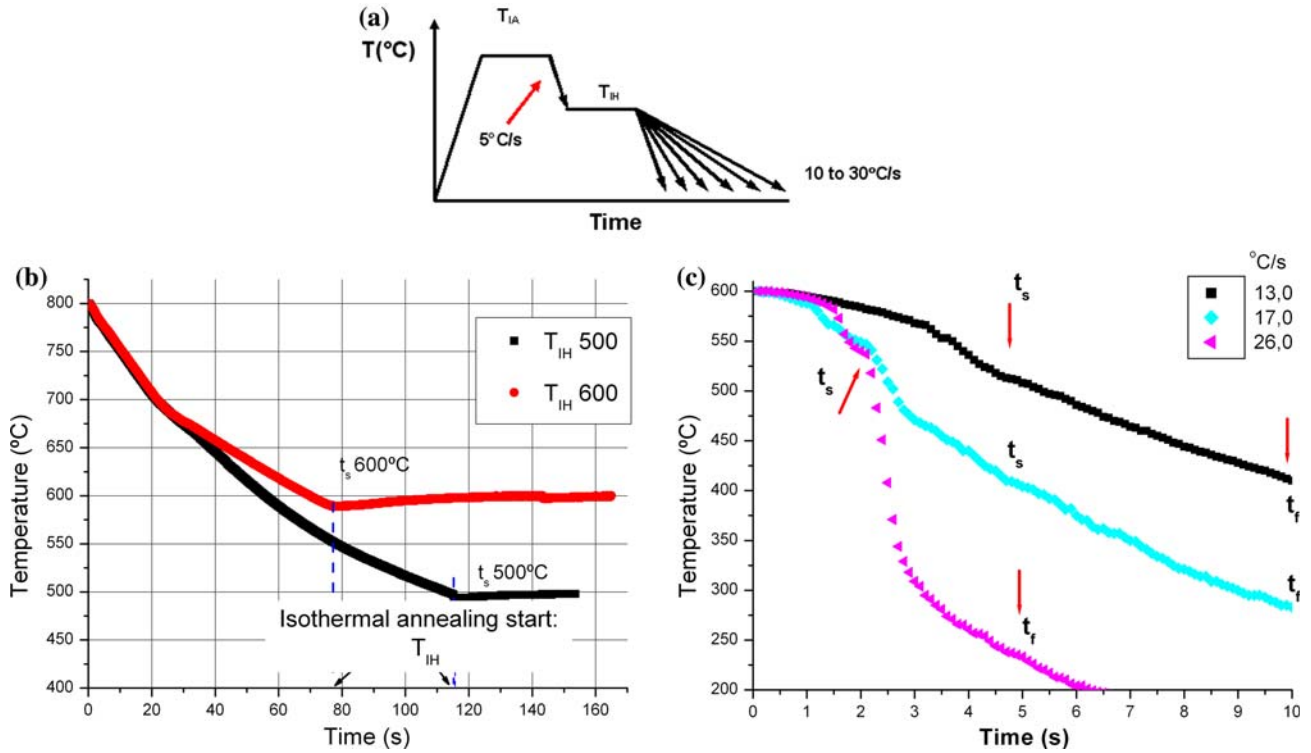

Fig. 1 Schematic diagram of thermal cycles simulation used in this work. T_{IA} is the intercritcal annealing temperatures and T_{IH} is isothermal hold temperature. Samples were cooled down at average rates between 10 and 30 °C s^{-1} from the isothermal hold temperature

Selected samples were studied using a Philips CM20 Transmission Electron Microscope (TEM). Thin foils for TEM study were prepared from mechanically ground to 0.25–0.3 mm slices. The 3 mm diameter discs were first punched out from the slices and then were electropolished in 5 wt.% perchloric acid in methanol using a twin-jet Tenupol unit, operating at 30 V and 0.2 A. The polishing solution was cooled to −20 to −30 °C using liquid nitrogen. TEM examination was carried out at 200 kV using bright field (BF), dark field, and selected aperture electron diffraction modes.

Measurements of volume fraction of constituents, as well as grain size, were made according to ASTM E 562-83 and ASTM E 112-88. The volume fraction was measured by point counting. The area of the ferrite grains was determined using an image system analysis and PRO-PLUS^{TM} software and the grain size was taken as a square root of its area. Vickers microhardness values were determined as a mean of 20 measurements made randomly on each polished specimen, using a 0.3 N load.

Results and discussion

Effect of annealing temperature

Figure 2 shows representative microstructures of samples cooled at 12 °C s^{-1} after isothermal holding at 600 °C. It could be seen that the higher the intercritical annealing temperature, the larger the volume fraction of austenite was available for transformation on cooling after annealing at 800 °C than at 740 °C. As a consequence, the microstructural characteristics developed in these samples could be summarized as follows:

(a) Cooling from 800 °C, Fig. 2a, b: The micrographs show a mixture of ferrite (gray phase) plus MA, represented here by light shades of gray and a few small particles of carbides, Fe_3C (black spots in Fig. 2a);
(b) Cooling from 760 °C, Fig. 2c, d: The microstructures show a slight increase in the ferrite volume fraction, when compared to the samples annealed at 800 °C. The volume fractions of MA constituent decrease and carbides increase, respectively. In addition, the small amount of pearlite was detected in the microstructure (Fig. 2d).
(c) Cooling from 740 °C, Fig. 2e, f: The trend described above continues. The volume fraction of ferrite continues to increase whereas the volume fractions of MA and carbides display the intermediate values between the ones for samples annealed at 800 and 760 °C. The amount of MA present decreases further whereas formation of carbides and pearlite colonies is also visible. At the same time, the size of ferrite grains does not increase appreciably due to growth restriction by the presence of carbides and MA that nucleate at grain boundaries of prior austenite.

These observations seem to indicate that high intercritical annealing temperatures lead to the formation of larger

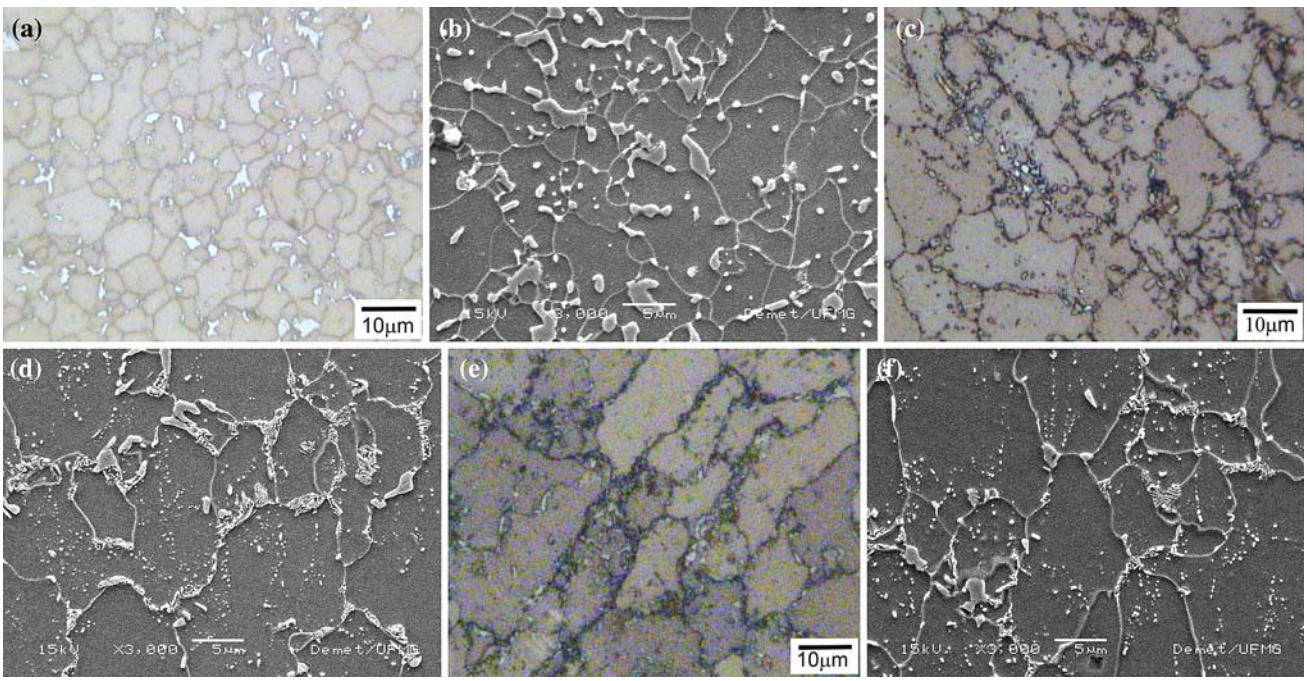

Fig. 2 Optical (**a**, **c**, and **e**) and scanning electron microscopy (**b**, **d**, and **f**) micrographs of samples after intercritical annealing at temperatures of 800 (**a**, **b**), 760 (**c**, **d**), and 740 °C (**e**, **f**). All samples were cooled at an average cooling rate of 12 °C s^{-1}

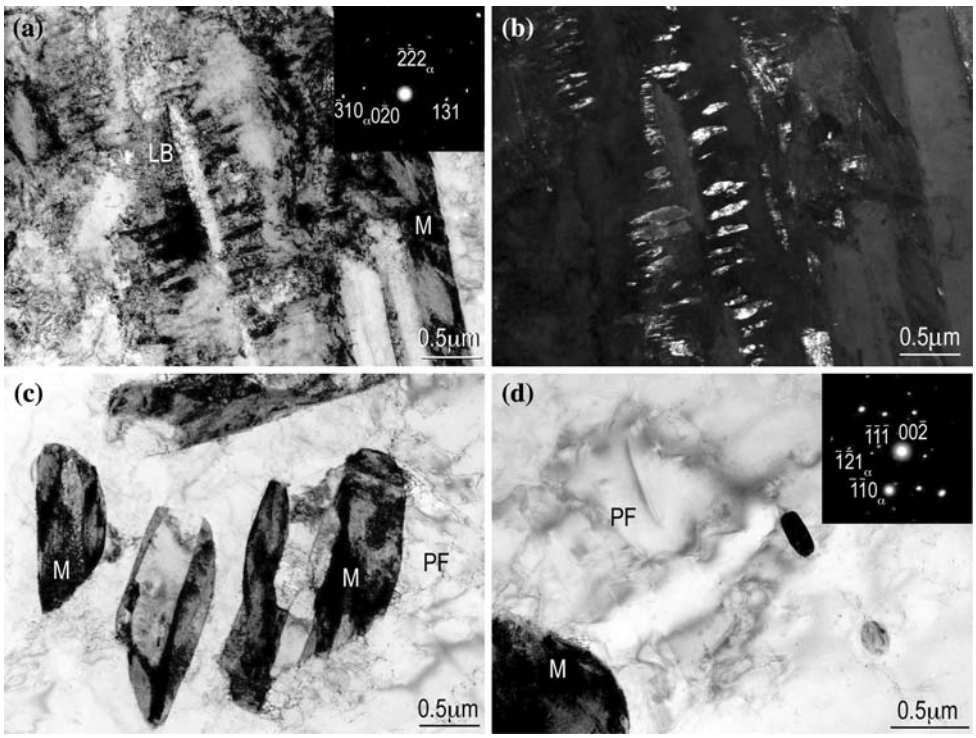

Fig. 3 TEM micrographs of steel after annealing at 800 °C for 300 s and cooling at 10 °C s^{-1} to room temperature. (**a**) Bright field (BF) image of lower bainite (LB). Insert is selected area electron diffraction (SAED) pattern with zone axis $[134]_\alpha//[\bar{1}01]$. (**b**) Dark field image showing cementite in lower bainite. (**c**) Bright field image of martensite islands in polygonal ferrite. (**d**) BF image of Fe_3C particles in polygonal ferrite. Inset is SAED with zone axis $[131]_\alpha//[\bar{1}10]$. PF denotes polygonal ferrite, M is martensite, LB is lower bainite, and α indicates bcc lattice

amounts of austenite than at lower temperatures. The amount of austenite after intercritical annealing at 800 °C has increased to 42% from 27% in the samples intercritically annealed at 740 °C. This austenite transforms to ferrite, iron carbides, and MA on cooling. As the annealing temperature is reduced, less austenite is available to transform on cooling resulting in a higher volume fraction of ferrite mixed with MA and Fe_3C [9]. In this case, colonies of pearlite are also present.

The effect of the intercritical annealing temperature on the microstructure could be followed in Figs. 3 and 4. The austenite starts from the pearlite colonies by nucleation at the cementite–ferrite interface followed by quick growth consuming the dissolving pearlite. Subsequently, austenite may nucleate at ferrite grain boundaries in competition with austenite growth from the prior pearlite colonies [10]. In general, higher annealing temperature and higher cooling rates result in higher volume fraction of hard constituents. The microstructure consists of a mixture of polygonal ferrite (PF), martensite, and lower bainite (LB). BF image of LB indicates the characteristic arrangement of parallel cementite particles within the bainitic ferrite plates (Fig. 3a, b). The PF contains relatively coarse (∼0.15 μm diameter/width) Fe_3C carbides of near spherical or elongated shapes (Fig. 3d). They might be the remains of the decomposed at annealing temperature pearlite and inherited by the recrystallized ferrite grains [11–13]. The martensite islands are result of transformation on cooling of formed during annealing austenite (Fig. 3c, d).

As the annealing temperature decreases (760 °C and cooling rate of 18 °C s^{-1}), more ferrite is remaining in the microstructure before cooling. Thus, less austenite transforms to MA. Some particles of Fe_3C appeared to be embedded within the PF grains. The microstructure of the samples heated to 760 °C contains predominantly PF with martensite islands and pearlite. Martensite was identified from TEM observation and has two morphologies: with high dislocation substructure and fine twinned martensite plates containing {112} type twins. By their turn, PF contains a significant number of coarse Fe_3C particles, which in some cases are remnants of decomposed pearlite, while in other cases are undissolved very coarse particles, formed probably during earlier stages of processing. Very fine spherical iron carbides (∼0.016 μm diameter) and a small amount of pearlite still could be found in the microstructure.

Figure 4 shows details of the microstructure of samples annealed at 740 °C and cooled down to room temperature at a rate of 20 °C s^{-1}. As annealing temperature drops further, the amount of ferrite increases and, it seems, remnants of decomposition of pearlite are also present. The micrographs show the presence of ferrite, martensite, some pearlite, and spherodised iron carbides within ferrite (Fig. 4a, c). This indicates that there was not enough time at this low annealing temperature for a significant amount of austenite to form resulting in formation of only small amount of MA. Formation of polygonised ferrite grains (Fig. 4b) indicates a recovery process taking place during annealing and isothermal holding [12].

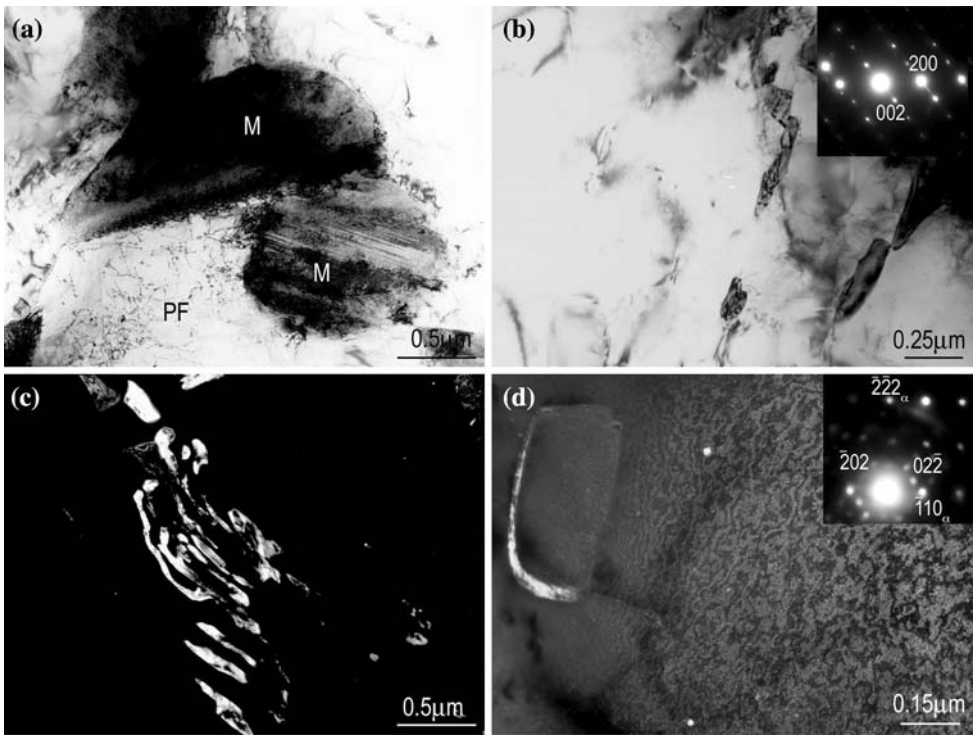

Fig. 4 TEM images of microstructure in samples annealed for 300 s at 740 °C and cooled at 20 °C s^{-1}. (**a**, **b**) Bright field image of martensite islands in polygonal ferrite and carbides. Inset in (**b**) is SAED from pearlite with zone axis $[\bar{1}3\bar{7}]_\alpha//[1\bar{2}1]$. (**c**) Dark field image of pearlite and isolated carbides. Inset in (**d**) is SAED from spheroidised Fe_3C, zone axis is $[5\bar{1}\bar{2}]$

It seems feasible at this stage to derive a trend of the dependence of the microstructure on the intercritical annealing temperature. A higher intercritical annealing temperature leads to a larger amount of austenite available to transformation at the end of intercritical annealing. Hence, the amount of pro-eutectoid ferrite will be reduced. The available austenite transforms then, on cooling, to iron carbides aggregates and MA. As the annealing temperature is lowered, less austenite is available to transform resulting in a higher volume fraction of proeutectoid ferrite, that is the old ferrite, and epitaxial ferrite that growth from previous one [14], these are mixed with smaller amounts of MA pools and Fe_3C. In this case, colonies of pearlite are also present.

Effect of the isothermal hold temperature

Comparing the microstructures developed in the samples after isothermal hold at 500 and 600 °C (Fig. 2), the similar effect of annealing temperature on the final microstructure could be seen, as discussed in the previous section. The microstructures of the samples annealed at the same temperatures, but subjected to various isothermal hold temperatures shows that amount of MA and Fe_3C decreases in the microstructure with lowering of isothermal hold temperature. This is due to the extending time for samples to reach the T_{IH}, during which some of the austenite transforms to PF (120 vs. 80 s for samples held at 500 and 600 °C, respectively). Other researchers [5, 13] observed similar trend. Thus, with decrease in T_{IH} the volume fractions of MA and carbides decrease and the amount of PF increases.

It is also worth noting that as the intercritical annealing decreases from 800 to 760 °C and then to 740 °C, the general trend observed in Fig. 2 is also reproduced for 500 °C isothermal transformed. In other words, as the T_{IA} decreases, the amount of austenite available to transformation at T_{IH} also decreases and the amount of pro-eutectoid ferrite increases. Thereby, less MA and Fe_3C are present.

Effect of cooling rate

Figure 5 shows a SEM micrograph for sample intercritically annealed at 760 °C and cooled to room temperature at an average rate of 28 °C s^{-1}. The effect of cooling rate on the microstructure could be seen from the comparison of the micrographs in Figs. 5 and 2, in which samples were subjected to 28 and 12 °C s^{-1} cooling from 760 °C, respectively. The micrographs show that when the cooling rate increases a larger volume fractions of MA and some discrete Fe_3C particles are visible in the microstructure (Fig. 5) compared to Fig. 2c, d. However, both constituents are also more dispersed in the matrix rather than situated at the ferrite grain boundaries, as seen in Fig. 2.

The microstructure for the case of samples heated to 760 °C and cooled at 28 °C s^{-1} consists of PF and martensite. Some Fe_3C particles are present in PF in the matrix

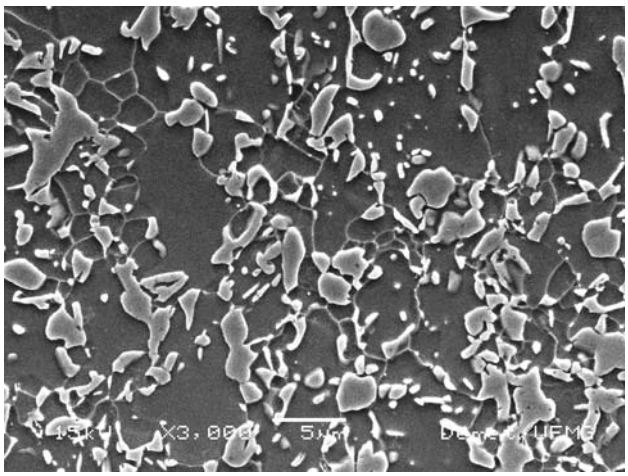

Fig. 5 SEM micrographs of the sample after intercritical annealing at 760 °C and cooling at an average cooling rate of 28 °C s^{-1}

and at the grain boundaries. Martensite again appears either containing a high dislocation density or fine twins, same as displayed in Figs. 3 and 4. Twinnned martensite forms on lowering the Ms temperature by alloying prior austenite with elements such as manganese or by increasing carbon content [15]. The present steel has a high concentration of Mn, which will diffuse to austenite during intercritical heating. The higher cooling rate seems to have suppressed pearlite formation, once the MA constituent remains in the microstructure, Fig. 5.

Effect on mechanical properties

Figure 6 shows the dependence of Vickers microhardness (HV) on the processing route. HV depends on MA volume fraction (roughly $\Delta HV = 4(\%\ MA)$) and cooling rate when the T_{IH} was 600 °C, Fig. 6a. This does not seem to be the case though for T_{IH} of 500 °C, Fig. 6b. This could be explained as follows. First, isothermal transformation at 600 °C implies an existence of a higher volume fraction of untransformed austenite than at 500 °C. This, in turn, transforms to ferrite and carbides or MA constituent, depending on the cooling rate applied. Lower volume fraction of MA present in the microstructure after isothermal hold at 500 °C results in reduced hardness (Fig. 6b). Second, as MA constituent and carbide particles have their volume fractions decreased at the lower T_{IH}, cooling rate becomes ineffective in altering hardness [5, 16, 17].

On the other hand, time available for austenite to ferrite transformation is the longest when the steel is annealed at 800 °C. This resulted in formation of more ferrite and carbides in detriment of forming MA during isothermal hold. This in turn, led to a significant reduction in hardness for these samples as compared to those intercritically annealed at lower temperatures (740–760 °C). This is why, the hardness values shown in Fig. 6a are the highest in the case of the samples annealed at 760 and 740 °C, isothermally held at 600 °C and cooled at the range of 20–30 °C s^{-1}, since these samples had also the highest volume fraction of MA constituent. The increase in strength with increasing of MA volume fraction has been confirmed by previous studies [5, 16].

Conclusions

The following conclusions can be drawn from the observations carried out in this work:

1. The intercritical annealing temperature affects the amounts of PF, MA constituents, Fe_3C, and pearlite

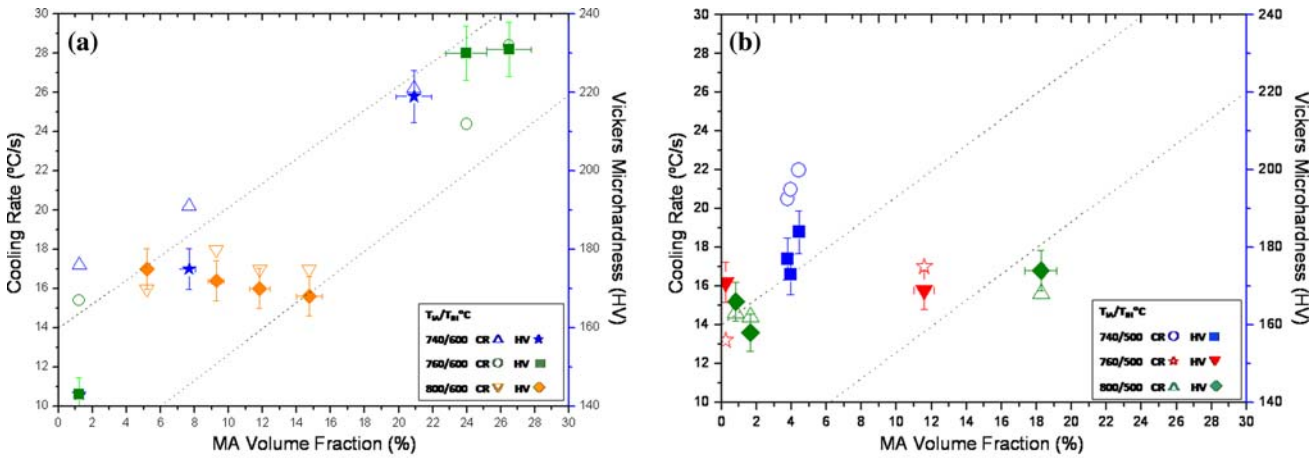

Fig. 6 Effect of the processing route on Vickers microhardness (*closed symbols*) and MA volume fraction for (**a**) $T_{IH} = 600$ °C and (**b**) $T_{IH} = 500$ °C. T_{IA} and T_{IH} are intercritical annealing and isothermal hold temperatures, respectively. CR denotes cooling rate (*open symbols*). *Dot lines* mean a tendency

present in the microstructure. The higher the temperature the higher will be the volume fraction of PF.
2. As the intercritical annealing temperature decreases, the amount of austenite available for transformation at isothermal hold temperature also decreases thereby decreasing the presence of MA and Fe_3C.
3. Higher cooling rates from isothermal hold temperatures to room temperature led to increase in the volume fraction of MA and Fe_3C, as expected. These constituents, however, were more dispersed in the matrix rather than located at the ferrite grain boundaries, as was the case for lower cooling rates.
4. The samples with high volume fractions of MA and carbides exhibit high Vickers microhardness.

References

1. Fekete JR (2005) In: Proc niobium microalloyed steel for automotive applications. Araxá, Brazil, TMS, p 107
2. DeArdo AJ (2003) Mater Sci Forum 426–432:49
3. Mesplont C, De Cooman BC (2002) Iron Steel 23:39
4. Lewellyn DT, Hillis DJ (1996) Iron Steelm 23:471
5. Pichler A, Traint S, Arnoldner G, Werner E, Pippan R, Stiaszny P (2000) In: Proc '42° mechanical working and steel processing', Toronto, Canada, October 22–25, p 573
6. Cota AB, Barbosa R, Santos DB (2000) J Mater Process Tech 100:156. doi:10.1016/S0924-0136(99)00467-7
7. Silva F, Lopes NIA, Santos DB (2006) Mater Charact 56:3. doi:10.1016/j.matchar.2005.07.008
8. Honeycombe RWK, Bhadeshia HKDH (1995) Steels, microstructure and properties, 2nd edn. Edward Arnold, London, England
9. Huang J, Poole WJ, Militzer M (2004) Metall Mater Trans A 35:3363. doi:10.1007/s11661-004-0173-x
10. Ramos LF, Matlock DK, Krauss G (1979) Metall Trans A 10:259. doi:10.1007/BF02817636
11. Speich GR, Demarest VA, Miller ML (1981) Metall Trans A 12:1419. doi:10.1007/BF02643686
12. Bunge H-J, Vlad CM, Kopp H-H (1984) Arch Eisenh 55:163
13. Estay S, Cheng L, Purdy GR (1984) Can Metall Q 23:121
14. Demir B, Erdoðan M (2008) J Mater Process Tech. doi:10.1016/j.jmatprotec.2007.12.094
15. Rao BVN, Rashid MS (1983) Metallography 16:19. doi:10.1016/0026-0800(83)90042-3
16. Qu J, Dabboussi W, Hassani F, Yue S (2005) ISIJ Int 45:1741. doi:10.2355/isijinternational.45.1741
17. Verdeja JI, PeroSanz JA, Asensio J (2005) Mater Sci Forum 500–501:429